Omega-Omega interaction from 2+1-flavor lattice quantum chromodynamics

doi: 10.1093/ptep/ptv091

PTEP

Prog. Theor. Exp. Phys. **2015**, 071B01 (9 pages)
DOI: 10.1093/ptep/ptv091

Letter

Omega-Omega interaction from 2+1-flavor lattice quantum chromodynamics

Masanori Yamada[1,*], Kenji Sasaki[2], Sinya Aoki[2,3], Takumi Doi[4], Tetsuo Hatsuda[4,5], Yoichi Ikeda[4], Takashi Inoue[6], Noriyoshi Ishii[7], Keiko Murano[7], and Hidekatsu Nemura[1,2] (on behalf of the HAL QCD Collaboration)

[1]*Graduate School of Pure and Applied Sciences, University of Tsukuba, Tsukuba 305-8571, Japan*
[2]*Center for Computational Sciences, University of Tsukuba, Tsukuba 305-8577, Japan*
[3]*Yukawa Institute for Theoretical Physics, Kyoto University, Kyoto 606-8502, Japan*
[4]*Theoretical Research Division, Nishina Center, RIKEN, Wako 351-0198, Japan*
[5]*Kavli IPMU (WPI), The University of Tokyo, Kashiwa, Chiba 277-8583, Japan*
[6]*Nihon University, College of Bioresource Sciences, Fujisawa 252-0880, Japan*
[7]*Research Center for Nuclear Physics (RCNP), Osaka University, Ibaraki 567-0047, Japan*
*E-mail: sinyamada@het.ph.tsukuba.ac.jp

Received March 13, 2015; Revised May 16, 2015; Accepted June 1, 2015; Published July 22, 2015

We investigate the interaction between Ω baryons in the $^1S_0$ channel from 2+1-flavor lattice quantum chromodynamics (QCD) simulations. On the basis of the HAL QCD method, the ΩΩ potential is extracted from the Nambu–Bethe–Salpeter wave function calculated on the lattice by using the PACS-CS gauge configurations with a lattice spacing of $a \simeq 0.09$ fm, a lattice volume of $L \simeq 2.9$ fm, and quark masses corresponding to $m_\pi \simeq 700$ MeV and $m_\Omega \simeq 1970$ MeV. The ΩΩ potential has a repulsive core at short distances and an attractive well at intermediate distances. Accordingly, the phase shift obtained from the potential shows moderate attraction at low energies. Our data indicate that the ΩΩ system with the present quark masses may appear close to the unitary limit where the scattering length diverges.

Subject Index B64, D32, D34

1. *Introduction* Strange dibaryons attract considerable interest both theoretically and experimentally in hadron physics. In particular, the H-dibaryon with (strangeness) $= -2$ [1] and the $N\Omega$ dibaryon with (strangeness) $= -3$ [2] are considered to be promising dibaryon states due to the absence of Pauli repulsions among valence quarks at short distances (see Refs. [3,4]). In recent years, the numerical and theoretical progress in lattice gauge theories has made it possible to attack such a problem directly from quantum chromodynamics (QCD) (see, e.g., Refs. [5–8] and references therein).

The purpose of this letter is to extend our previous work on (strangeness) $= -2$ systems, such as the H-dibaryon [5,6] and $N\Xi$ [9], and (strangeness) $= -3$ systems, such as $N\Omega$ [10], to the (strangeness) $= -6$ ΩΩ system in 2+1-flavor lattice QCD. In our approach (the HAL QCD method), the baryon–baryon potential is extracted from the Nambu–Bethe–Salpeter (NBS) wave function calculated on the lattice: Such a potential deduced in lattice QCD is guaranteed to reproduce physical observables (e.g. the scattering phase shift) by construction [11,12]. The HAL QCD method has

Funded by SCOAP[3]

several advantages over the conventional finite-volume method [13]: (i) The finite-volume effect is highly suppressed due to the short-range character of baryon potentials, (ii) ground-state saturation of the two-particle system is not required for extracting the potential, since the same potential dictates all the scattering states on the lattice, and (iii) the physics behind the baryon–baryon interaction can be easily grasped from the spatial structure of the potential. Further details on these points are discussed in Refs. [14,15].

So far, there exist several investigations on the ΩΩ interaction using phenomenological quark models: Some studies show strong attraction, which may cause an ΩΩ bound state [16,17], while other studies show weak repulsion [18,19]. A recent lattice QCD analysis of the ΩΩ scattering length [20] by using the standard finite-volume method [13] shows weak repulsion in the S-wave scattering with a scattering length $a_{\Omega\Omega} = -0.16 \pm 0.22$ fm: This indicates that the ΩΩ system is unlikely to have a strongly bound dibaryon, although the large error prevents us from making a firm conclusion about the details of the interaction.

2. *The HAL QCD potential* Let us first recapitulate the essential part of the HAL QCD method to be used for extracting the ΩΩ potential. The basic quantity is the equal-time NBS wave function with the Euclidean time t,

$$\psi^W_{\alpha k,\beta l}(\vec{r})e^{-Wt} \equiv \left\langle 0|\Omega_{\alpha,k}(t,\vec{r})\Omega_{\beta,l}(t,\vec{0})|\Omega\Omega, W\right\rangle, \tag{1}$$

where $|\Omega\Omega, W\rangle$ is an exact (strangeness)=−6 state with zero total momentum. The total energy of the system is given by $W = 2\sqrt{m_\Omega^2 + \vec{p}^2}$ with the Ω baryon mass m_Ω and the relative momentum $\vec{p}$. The local interpolating operators for the Ω baryon, $\Omega(x)$ and $\overline{\Omega}(x)$, are taken to be

$$\begin{aligned}\Omega_{\alpha,k}(x) &\equiv \varepsilon^{abc} s_a^T(x) C\gamma_k s_b(x) s_{c,\alpha}(x),\\ \overline{\Omega}_{\alpha,k}(x) &\equiv \Omega^\dagger_{\alpha,k}\gamma^0 = -\varepsilon^{abc}\overline{s}_{a,\alpha}(x)\overline{s}_b(x)\gamma_{k_1} C\overline{s}_c^T(x),\end{aligned} \tag{2}$$

where a, b, and c are color indices, ε^{abc} is the totally anti-symmetric tensor, γ_k represents the Dirac matrix, and α is the spinor index. The charge-conjugation matrix is taken as $C \equiv \gamma_4\gamma_2 = -C^{-1} = -C^T = -C^\dagger$ in the Euclidean space.

An important property of the NBS wave function is its asymptotic behavior at long distances, denoted simply as

$$\psi^W(\vec{r}) \sim \sum_{L,M} e^{i\delta_L(p)} \frac{\sin\left(pr - \frac{L\pi}{2} + \delta_L(p)\right)}{pr} C_{L,M} Y_{LM}(\vec{\Omega}), \tag{3}$$

where $p = |\vec{p}|$, $r = |\vec{r}|$, $\vec{\Omega}$ is the solid angle of $\vec{r}$, Y_{LM} is the spherical harmonic function, and L is the orbital angular momentum. Although Eq. (3) looks like a quantum mechanical formula, it can be derived from the unitarity of the S-matrix in quantum field theory with $\delta_L(p)$ being the scattering phase shift for given quantum numbers in QCD [11,12].

Our next task is to define the potential from which this scattering phase shift can be calculated. In the HAL QCD method, such a potential is defined through a Schrödinger-type equation,

$$(E - H_0)\psi^W(\vec{r}) = \int d^3r' U(\vec{r},\vec{r}')\psi^W(\vec{r}'), \tag{4}$$

where $H_0 \equiv -\frac{1}{2\mu_\Omega}\nabla^2$ is the free Hamiltonian, $\mu_\Omega \equiv m_\Omega/2$ is the reduced mass, and $E \equiv \frac{1}{2\mu_\Omega}p^2$ is the kinetic energy. Here $U(\vec{r},\vec{r}')$ is the non-local but energy-independent potential, which can be

expanded in terms of the non-locality (the velocity or derivative expansion) [21]. The convergence of the velocity expansion at low energies has been investigated previously for nucleon–nucleon scattering [22] and pion–pion scattering [23]. Since we consider low-energy S-wave scattering far below the meson production threshold in this letter, we take only the leading-order local potential, $V(\vec{r})$, in the expansion: $U(\vec{r},\vec{r}') = V(\vec{r})\delta(\vec{r}-\vec{r}') + \mathcal{O}(\vec{\nabla})$.

Note that $V(\vec{r})$ is an effective central potential, which contains not only a genuine central part but also, implicitly, a tensor part [11,12].

The NBS wave function can be extracted from the asymptotic temporal behavior of the four-point (4-pt) function,

$$\begin{aligned} F(\vec{r}, t-t_0) &= \left\langle 0|\Omega(t,\vec{r})\Omega(t,\vec{0})\mathcal{J}(t_0)|0\right\rangle \\ &= \sum_n \left\langle 0|\Omega(t,\vec{r})\Omega(t,\vec{0})|\Omega\Omega, W_n\right\rangle \langle \Omega\Omega, W_n|\mathcal{J}(t_0)|0\rangle + \cdots \\ &= \sum_n a_n \psi^{W_n}(\vec{r}) e^{-W_n(t-t_0)} + \cdots \simeq a_0 \psi^{W_0}(\vec{r}) e^{-W_0(t-t_0)}, \quad (t-t_0 \to \infty), \end{aligned} \tag{5}$$

where $\mathcal{J}(t_0)$ is the wall-source operator that creates the $\Omega\Omega$ state at t_0, a_n is the matrix element defined by $\langle \Omega\Omega, W_n|\mathcal{J}(0)|0\rangle$, W_n are discrete QCD eigenenergies in the finite volume below the inelastic threshold, and W_0 is the lowest eigenenergy. The ellipses in the above equation represent inelastic contributions in the $\Omega\Omega$ system, which are suppressed for large $t-t_0$.

Equation (5) shows that the NBS wave function for the ground state can be extracted from the 4-pt function at large t, as long as other contributions from $W_{n\geq 1} > W_0$ can be neglected. In practice, however, the increasing statistical errors of the 4-pt function at large t make it difficult to achieve ground-state saturation with reasonable accuracy [24]. Moreover, as the volume increases, larger and larger t becomes necessary to extract $\psi^{W_0}(\vec{r})$. These problems can be simultaneously avoided by the time-dependent HAL QCD method introduced in Ref. [14], where we start with the so-called R-correlator,

$$R(\vec{r}, t-t_0) \equiv \frac{F(\vec{r}, t-t_0)}{e^{-2m_\Omega(t-t_0)}} = \sum_n a_n \psi^{W_n}(\vec{r}) e^{-\Delta W_n(t-t_0)} + \cdots, \tag{6}$$

with $\Delta W_n = W_n - 2m_\Omega$. Since $\Delta W_n = \frac{\vec{p}_n^{\,2}}{m_\Omega} - \frac{\Delta W_n^2}{4m_\Omega}$, we have

$$\begin{aligned} -\frac{\partial}{\partial t} R(\vec{r}, t) &\simeq \sum_n \Delta W_n a_n \psi^{W_n}(\vec{r}) e^{-\Delta W_n t} = \sum_n \left(\frac{\vec{p}_n^{\,2}}{m_\Omega} - \frac{1}{4m_\Omega}\frac{\partial^2}{\partial t^2} \right) a_n \phi^{W_n}(\vec{r}) e^{-\Delta W_n t} \\ &= \left(-\frac{1}{m_\Omega}\nabla^2 - \frac{1}{4m_\Omega}\frac{\partial^2}{\partial t^2} \right) R(\vec{r}, t) + \int d^3r' U(\vec{r}, \vec{r}') R(\vec{r}', t), \end{aligned} \tag{7}$$

where we have replaced $\vec{p}_n^{\,2}/m_\Omega$ by $U - \nabla^2/m_\Omega$ using Eq. (4). We then arrive at the time-dependent equation,

$$\left(\frac{1}{m_\Omega}\nabla^2 - \frac{\partial}{\partial t} + \frac{1}{4m_\Omega}\frac{\partial^2}{\partial t^2} \right) R(\vec{r}, t) \simeq \int d^3r' U(\vec{r}, \vec{r}') R(\vec{r}', t), \tag{8}$$

where "$\simeq$" implies that we have neglected inelastic contributions by taking sufficiently large $t-t_0$. Equation (8) gives $U(\vec{r}, \vec{r}')$ directly from $F(\vec{r}, t)$. This method no longer requires ground-state saturation, so that the moderately large values of $t-t_0$ that suppress inelastic contributions are enough

Table 1. The relation between conserved quantum numbers (J and P) and quantum numbers in the asymptotic $\Omega\Omega$ channel.

	$P=+$	$P=-$
$J=0$	${}^1S_0, {}^5D_0$	${}^3P_0, {}^7F_0$
$J=1$	${}^5D_1$	${}^3P_1, {}^7F_1$
$J=2$	${}^5S_2, {}^1D_2, {}^5D_2, {}^5G_2$	${}^3P_2, {}^7P_2, {}^3F_2, {}^7F_2, {}^7H_2$
$J=3$	${}^5D_3, {}^5G_3$	${}^7P_3, {}^3F_3, {}^7F_3, {}^7H_3$
$J=4$	${}^5D_4, {}^1G_4, {}^5G_4, {}^5I_4$	${}^7P_4, {}^3F_4, {}^7F_4, {}^3H_4, {}^7H_4, {}^7J_4$

for reliable extraction of the potential. Then, in the leading order of the velocity expansion, we obtain

$$V(\vec{r}) = \frac{\left(\frac{1}{m_\Omega}\nabla^2 - \frac{\partial}{\partial t} + \frac{1}{4m_\Omega}\frac{\partial^2}{\partial t^2}\right) R(\vec{r},t)}{R(\vec{r},t)}. \tag{9}$$

3. *Interpolating operators for the $\Omega\Omega$ system* The present system can be characterized by the total spin (S), the orbital angular momentum (L), the total angular momentum (J), and the parity P. The asymptotic $\Omega\Omega$ state with given L and S has a factor $(-1)^{S+L+1}$ under the exchange of two Ω, so that $S+L$ must be even due to the Fermi statistics of Ω baryons. In Table 1, we show low-J channels ${}^{2S+1}L_J$, which appear for given conserved quantum numbers J and P. In this letter, we employ the wall source, $L=0$ with $S=0$ at $t=t_0$, which creates the $J^P=0^+$ state, so that only the upper-left corner of this table is considered. Then, both ${}^1S_0$ and ${}^5D_0$ channels appear after the QCD interactions at $t>t_0$. As mentioned before, we determine only the effective central potential from the ${}^1S_0$ channel at $t>t_0$, where the effects of the ${}^5D_0$ state are implicitly included.

The interpolating operators for Ω with $S=3/2$ and $S_z=\pm 3/2, \pm 1/2$ read

$$\Omega_{\frac{3}{2},\frac{3}{2}} = -(\psi\Gamma_+\psi)\psi_{\frac{1}{2}}, \tag{10}$$

$$\Omega_{\frac{3}{2},\frac{1}{2}} = \frac{1}{\sqrt{3}}\left[\sqrt{2}(\psi\Gamma_Z\psi)\psi_{\frac{1}{2}} + (\psi\Gamma_+\psi)\psi_{-\frac{1}{2}}\right], \tag{11}$$

$$\Omega_{\frac{3}{2},-\frac{1}{2}} = \frac{1}{\sqrt{3}}\left[\sqrt{2}(\psi\Gamma_Z\psi)\psi_{-\frac{1}{2}} + (\psi\Gamma_-\psi)\psi_{\frac{1}{2}}\right], \tag{12}$$

$$\Omega_{\frac{3}{2},-\frac{3}{2}} = (\psi\Gamma_-\psi)\psi_{-\frac{1}{2}}, \tag{13}$$

where $\Gamma_\pm \equiv \frac{1}{2}\left(C\gamma^2 \pm iC\gamma^1\right)$ and $\Gamma_Z \equiv \frac{-i}{\sqrt{2}}C\gamma^3$. We take only the upper two components in the Dirac representation for the quark operators, so that the Ω operator does not have the $S=1/2$ component. Combining these operators, the interpolating operators for the $\Omega\Omega$ system with the total spin $S=3,2,1,0$ with $S_z=0$ are given by

$$(\Omega\Omega)_{0,0} = \frac{1}{2}\left(\Omega_{\frac{3}{2},\frac{3}{2}}\Omega_{\frac{3}{2},-\frac{3}{2}} - \Omega_{\frac{3}{2},\frac{1}{2}}\Omega_{\frac{3}{2},-\frac{1}{2}} + \Omega_{\frac{3}{2},-\frac{1}{2}}\Omega_{\frac{3}{2},\frac{1}{2}} - \Omega_{\frac{3}{2},-\frac{3}{2}}\Omega_{\frac{3}{2},\frac{3}{2}}\right). \tag{14}$$

In this letter, we use Eq. (14) to calculate the $S=0$, $S_z=0$ state.

To extract the $L=0$ state at the sink t on the lattice, we employ the cubic-group projection defined by

$$P^a_\nu = \frac{d_a}{g}\sum_i^g D^a_{\nu\nu}(R_i)^* R_i, \tag{15}$$

where a represents an irreducible representation of the cubic group with the dimension of the representation d_a, R_i is an element of the cubic group acting on $\vec{r}$ of Ω operators, $D^a(R_i)$ is the

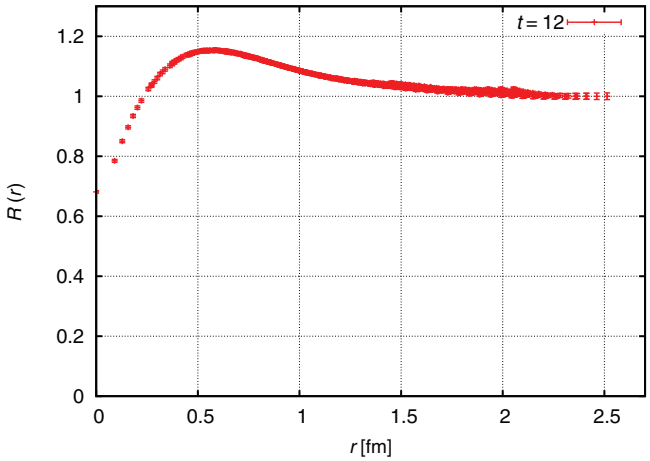

Fig. 1. The R-correlator in the ${}^1S_0$ channel as a function of the relative distance r for $t - t_0 = 12$.

corresponding matrix in the irreducible representation acting on the spin of Ω operators, and g is the order of the cubic group. We use the A_1 projection, which generates the $L = 0$ as well as the $L = 4, 6, \ldots$ states, where the $L = 4, 6, \ldots$ components are expected to be negligibly small. For example, we have

$$P^{A_1}(\Omega\Omega)_{0,0}(\vec{r}) = \frac{1}{24}\sum_{i=1}^{24}\Omega_{0,0}(R_i\vec{r}). \tag{16}$$

4. *The* $\Omega\Omega$ *potential* We employ 399 gauge configurations generated by the PACS-CS Collaboration with the renormalization-group-improved gauge action and the non-perturbatively $\mathcal{O}(a)$-improved Wilson quark action in 2+1-flavor QCD [25]. These configurations were obtained at $\beta = 1.90$ ($a = 0.0907(13)$ fm) on a $32^3 \times 64$ lattice, whose physical extension is $L = 2.9$ fm, with the hopping parameters $\kappa_{ud} = 0.137\,00$ and $\kappa_s = 0.136\,40$, corresponding to $m_\pi = 701(5)$ MeV and $m_\Omega = 1966(6)$ MeV. We employ the wall quark-source with Coulomb gauge fixing. The periodic (Dirichlet) boundary condition is imposed in the spatial (temporal) direction. To improve the statistics, we perform the measurement at 64 source time slices for each configuration, where the unified contraction algorithm [26] is used to calculate the NBS wave functions. Statistical errors are estimated by the jackknife method. We make analyses with bin sizes of 1, 3, 7, 19, 21, and 57, and the bin-size dependence is found to be negligible. Hereafter, we show the results obtained with a bin size of 1, unless otherwise indicated.

Figure 1 shows the R-correlator (Eq. (6)) in the ${}^1S_0$ channel as a function of r for $t - t_0 = 12$, where the R-correlator is normalized to 1 at $r = 2.5$ fm. We find that the R-correlator is enhanced at intermediate distances, while it is suppressed at short distances. The latter behavior is consistent with partial Pauli blocking at the quark level, similar to situations in the nucleon–nucleon force [15].

Shown in Fig. 2 is the effective central potential $V_c(r)$ between Ω baryons at $t - t_0 = 12$ in the ${}^1S_0$ channel. The Laplacian term and the time-derivative term calculated from the R-correlator on the right-hand side of Eq. (8) are separately plotted in the figure, together with the total potential. We here approximate the time-derivative term in Eq. (9) by $\frac{\partial}{\partial t}R(t) = \frac{R(t+1)-R(t-1)}{2}$ and $\frac{\partial^2}{\partial t^2}R(t) = R(t+1) + R(t-1) - 2R(t)$. We find that the time-derivative terms make sizable contributions to the total potential: The 1st derivative in t dominates over the 2nd derivative in t. The

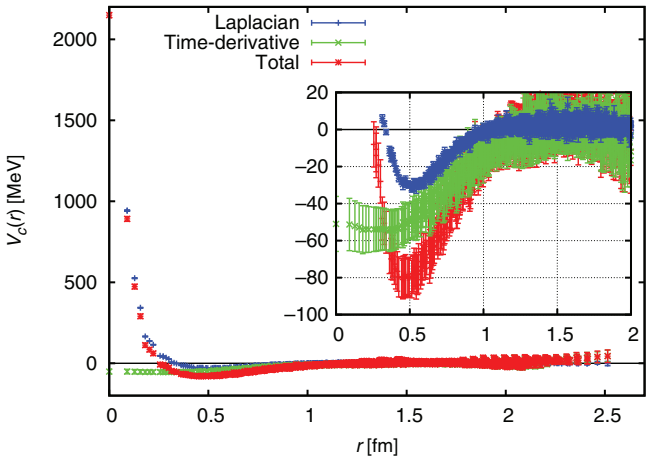

Fig. 2. The effective central potential for the ΩΩ system in the $^1S_0$ channel at $t - t_0 = 12$. We plot the Laplacian term (blue), the time-derivative term (green), and the total (red) separately.

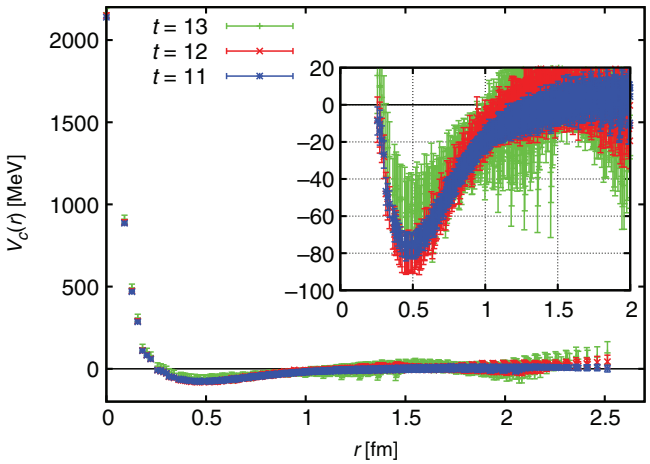

Fig. 3. The effective central potential $V_c(r)$ in the $^1S_0$ channel at $t - t_0 = 11$ (blue), 12 (red), 13 (green).

latter, corresponding to the relativistic effect, is negligible. Figure 3 shows the time dependence of $V_c(r)$ at $t - t_0 = 11, 12, 13$. This particular region of t is chosen to suppress contamination from excited states in the single Ω propagator at smaller t and simultaneously to avoid statistical errors at larger t. We observe that the potential is nearly independent of t within statistical errors, as expected in the time-dependent method [14].

The effective central potential $V_c(r)$ in Fig. 3 has a repulsive core at short distances and an attractive well at intermediate distances. The short-distance repulsion may be attributed to the color magnetic interaction rather than Pauli blocking from the viewpoint of the quark model [27–29]. One the other hand, meson-exchange effects including scalar and pseudo-scalar mesons with $s\bar{s}$ components may be responsible for the attraction at intermediate distances. To make such physical interpretations, further studies on the quark-mass dependence of the ΩΩ potential would be necessary.

5. *The ΩΩ phase shift* To obtain the S-wave phase shift, we fit the potential in Fig. 3 using a function that contains two Gaussian terms plus the Yukawa squared term with a form factor [15],

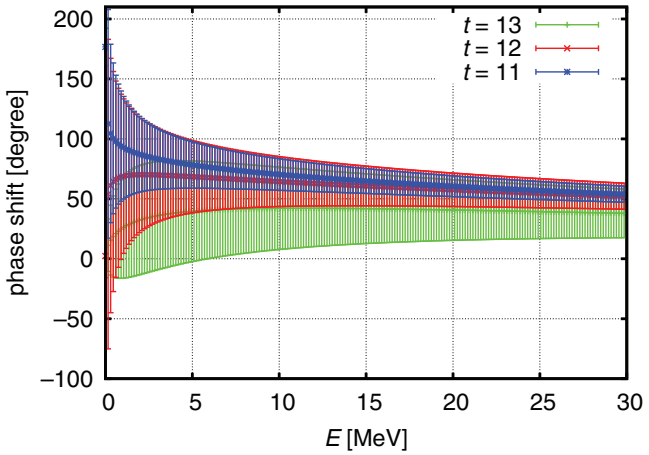

Fig. 4. Phase shift $\delta_0(k)$ of the ΩΩ in the $(^1S_0)$ channel at $t - t_0 = 11$ (blue), 12 (red), 13 (green).

given by

$$V_c(r) = a_1 e^{-a_2 r^2} + a_3 e^{-a_4 r^2} + a_5 \left(1 - e^{-a_6 r^2}\right)^2 \left(\frac{e^{-a_7 r}}{r}\right)^2, \quad \lim_{r\to 0} V(r) = a_1 + a_3. \tag{17}$$

This 2 Gauss + (Yukawa)^2 form gives a fairly good fit with $\chi^2/\text{d.o.f.} \sim 0.50$ at $t - t_0 = 12$. The resulting parameters are $a_1 = 1.69(6) \times 10^3$ MeV, $a_2 = 1.24(3) \times 10^2\,\text{fm}^{-2}$, $a_3 = 4.44(68) \times 10^2$ MeV, $a_4 = 5.68(1.31)\,\text{fm}^{-2}$, $a_5 = -7.06(14.64) \times 10^4$ MeV, $a_6 = 6.25(5.77) \times 10^{-1}\,\text{fm}^{-2}$, $a_7 = 3.43(30)\,\text{fm}^{-1}$ at $t - t_0 = 12$.

Using the fitted potential, we solve the Schrödinger equation in the infinite volume to calculate the scattering phase shift $\delta_L(k)$ of the ΩΩ system in the $^1S_0$ channel by the formula with $L = 0$,

$$\tan\delta_L(k) = \lim_{x_1,x_2\to\infty} \frac{\psi_k(x_2)\sin\left(kx_1 - \frac{L\pi}{2}\right) - \psi_k(x_1)\sin\left(kx_2 - \frac{L\pi}{2}\right)}{\psi_k(x_1)\cos\left(kx_2 - \frac{L\pi}{2}\right) - \psi_k(x_2)\cos\left(kx_1 - \frac{L\pi}{2}\right)}, \tag{18}$$

where ψ_k is the wave function and k is the magnitude of the momentum.

Figure 4 shows the phase shift as a function of the kinetic energy, $E = k^2/m_\Omega$. The result indicates that the ΩΩ interaction is attractive at low energies, while the existence of the bound state is inconclusive because of large statistical errors near $k = 0$. Indeed, the central value of $\delta_0(k = 0)$ at $t - t_0 = 11$ is 180°, while it becomes zero at $t - t_0 = 12$, 13. Due to the same reason, the scattering length and the effective range cannot be extracted reliably from this phase shift. A possible physical interpretation of such a situation is that the ΩΩ system at the present quark masses may appear close to the unitary limit, where the scattering length diverges and changes its sign.

6. *Conclusion* In this letter, we have calculated the effective central potential and the scattering phase shift between Ω baryons in the $^1S_0$ channel by using the HAL QCD method. We have found that the ΩΩ potential has short-range repulsion and intermediate-range attraction just like the nucleon–nucleon potential. The short-range repulsion of this system is a reflection of the partial Pauli blocking at the quark level, similar to the nucleon–nucleon potential, and is in contrast to the cases of the H-dibaryon or $N\Omega$ system with no repulsion. The ΩΩ interaction is attractive at low energies, but is not strong enough to form a tightly bound dibaryon at quark masses corresponding to $m_\pi \simeq 700$ MeV and $m_\Omega \simeq 1970$ MeV. Rather, the system may appear close to the unitary limit at these quark masses. We plan to carry out 2+1-flavor simulations at the physical quark masses, in order to investigate

whether the attraction found in the present study increases or decreases toward the physical quark masses.

Acknowledgements

We are grateful to the authors and maintainers of CPS++ [30], a modified version of which is used for the simulations done in this work. We thank the PACS-CS Collaboration and ILDG/JLDG for providing us with the 2+1-flavor gauge configurations [31]. The numerical computations for this work were carried out on the KEK supercomputer system (BG/Q) under JICFuS-H26-3 and on local machines at the University of Tsukuba. This work is supported in part by a Grant-in-Aid of the Ministry of Education, Culture, Sports, Science and Technology (Nos. 20340047, 22540268, 19540261, (B)25287046, (C)26400281, 24740146), the Strategic Program for Innovative Research (SPIRE) Field 5, and JICFuS [32]. T.H. was partially supported by the RIKEN iTHES Research Group.

Funding

Open Access funding: SCOAP[3].

References

[1] R. L. Jaffe, Phys. Rev. Lett. **38**, 195 (1977).
[2] J. T. Goldman, K. Maltman, G. J. Stephenson, Jr., K. E. Schmidt, and F. Wang, Phys. Rev. Lett. **59**, 627 (1987).
[3] M. Oka, Phys. Rev. D **38**, 298 (1988).
[4] A. Gal, in *From Nuclei to Stars: Festschrift in Honor of Gerald E. Brown* ed. S. Lee (World Scientific, Singapore, 2011), pp. 157–170 [arXiv:1011.6322 [nucl-th]] [Search INSPIRE].
[5] T. Inoue et al. [HAL QCD Collaboration], Nucl. Phys. A **881**, 28 (2012) [arXiv:1112.5926 [hep-lat]] [Search INSPIRE].
[6] K. Sasaki [HAL QCD Collaboration], Nucl. Phys. A **914**, 231 (2013).
[7] S. R. Beane et al. [NPLQCD Collaboration], Phys. Rev. D **85**, 054511 (2012) [arXiv:1109.2889 [hep-lat]] [Search INSPIRE].
[8] J. Haidenbauer, U. G. Meisner, and S. Petschauer, Eur. Phys. J. A **51**, 17 (2015) [arXiv:1412.2991 [nucl-th]] [Search INSPIRE].
[9] H. Nemura, N. Ishii, S. Aoki, and T. Hatsuda, Phys. Lett. B **673**, 136 (2009) [arXiv:0806.1094 [nucl-th]] [Search INSPIRE].
[10] F. Etminan et al. [HAL QCD Collaboration], Nucl. Phys. A **928**, 89 (2014) [arXiv:1403.7284 [hep-lat]] [Search INSPIRE].
[11] N. Ishii, S. Aoki, and T. Hatsuda, Phys. Rev. Lett. **99**, 022001 (2007).
[12] S. Aoki, T. Hatsuda, and N. Ishii, Prog. Theor. Phys. **23**, 89 (2010) [arXiv:0909.5585 [hep-lat]] [Search INSPIRE].
[13] M. Lüscher, Nucl. Phys. B **354**, 531 (1991).
[14] N. Ishii et al. [HAL QCD Collaboration], Phys. Lett. B **712**, 437 (2012) [arXiv:1203.3642 [hep-lat]] [Search INSPIRE].
[15] S. Aoki et al. [HAL QCD Collaboration], Prog. Theor. Exp. Phys. **2012**, 01A105 (2012) [arXiv:1206.5088 [hep-lat]] [Search INSPIRE].
[16] Z. Y. Zhang, Y. W. Yu, C. R. Ching, T. H. Ho, and Z.-D. Lu, Phys. Rev. C **61**, 065204 (2000).
[17] Z. Y. Zhang, Y. W. Yu, P. N. Shen, L. R. Dai, A. Faessler, and U. Straub, Nucl. Phys. A **625**, 59 (1997).
[18] F. Wang, J. Ping, G. Wu, L. Teng, and T. Goldman, Phys. Rev. C **51**, 3411 (1995).
[19] F. Wang, G. Wu, L. Teng, and T. Goldman, Phys. Rev. Lett. **69**, 2901 (1992).
[20] M. I. Buchoff, T. C. Luu, and J. Wasem, Phys. Rev. D **85**, 094511 (2012) [arXiv:1201.3596 [hep-lat]] [Search INSPIRE].
[21] S. Okubo and R. E. Marshak, Ann. Phys. **4**, 166 (1958).
[22] K. Murano et al. [HAL QCD Collaboration], Prog. Theor. Phys. **125**, 1225 (2011) [arXiv:1012.3814v1 [hep-lat]].
[23] T. Kurth, N. Ishii, T. Doi, S. Aoki, and T. Hatsuda, J. High Energy Phys. **1312**, 015 (2013) [arXiv:1305.4462 [hep-lat]] [Search INSPIRE].

[24] G. P. Lepage, in *Actions to Answers: Proceedings of the TASI 1989*, eds. T. Degrand and D. Toussaint (World Scientific, Singapore, 1990).
[25] S. Aoki et al. [PACS-CS Collaboration], Phys. Rev. D **79**, 034503 (2009).
[26] T. Doi and M. G. Endres, Comput. Phys. Commun. **184**, 117 (2013).
[27] M. Oka and K. Yazaki, Prog. Theor. Phys. **66**, 556 (1981).
[28] M. Oka and K. Yazaki, Prog. Theor. Phys. **66**, 572 (1981).
[29] M. Oka and K. Yazaki, Phys. Lett. B **90**, 41 (1980).
[30] Physics Columbia System (CPS), http://qcdoc.phys.columbia.edu/cps.html.
[31] ILDG/JLDG, http://www.jldg.org.
[32] Institute Joint for Computational Fundamental Science, http://www.jicfus.jp.